

Dynamic Control Allocation for Damping of Inter-Area Oscillations

M. Ehsan Raoufat ^{ID}, Student Member, IEEE, Kevin Tomsovic, Fellow, IEEE, and Seddik M. Djouadi, Member, IEEE

Abstract—Use of actuator redundancy to achieve higher reliability is a widely accepted engineering design technique and is used in this study to build resiliency and ensure power system stability in the presence of high levels of renewables. This paper presents a new design method for fault-tolerant wide-area damping controllers (WADCs) using modal-based control allocation (MB-CA), which coordinates a set of actuators to contribute to damping of inter-area oscillations. In our proposed method, when an actuator fails or is unavailable (e.g., due to communication failure), the supervisory MB-CA distributes the control signals to the remaining healthy actuators based on effects on the modal system, desired control actions, and actuator constraints. Our proposed block offers the benefits of modular design where it is independent of the nominal WADC. The proposed method consists of mainly two design steps. The first step is to design a WADC based on a fault-free model using robust control methods. The second step is to design an MB-CA to manage actuator availability and constraints. To validate the feasibility and demonstrate the design principles, a set of comprehensive case studies are conducted on a modified 192-bus Western Electricity Coordinating Council system. Numerical results verify the effectiveness of the proposed approach in ensuring resiliency to different actuator failures and actuator availability.

Index Terms—Low-frequency oscillations, damping controller, fault-tolerant control, modal-based control allocation, WECC.

NOMENCLATURE

δ	Rotor angle.
ω, ω_s	Rotor and synchronous speed.
H	Rotor inertia coefficient.
D	Damping coefficient.
E'_d, E'_q	d -axis and q -axis transient voltage.
T'_{d0}, T'_{q0}	d -axis and q -axis transient time constant.
I_d, I_q	d -axis and q -axis armature current.
X_d, X_q	d -axis and q -axis reactance of the generator.
X'_d, X'_q	d -axis and q -axis transient reactance of the generator.
T_M	Mechanical torque.
E_{fd}	Exciter field voltage.

Manuscript received September 23, 2016; revised February 6, 2017; accepted March 4, 2017. Date of publication March 23, 2017; date of current version October 18, 2017. This work was supported in part by the National Science Foundation under Grant CNS-1239366, in part by the Engineering Research Center Program of the National Science Foundation and the Department of Energy under NSF Award EEC-1041877, and in part by the CURENT Industry Partnership Program. Paper no. TPWRS-01434-2016. (Corresponding author: M. Ehsan Raoufat.)

The authors are with the Min H. Kao Department of Electrical Engineering and Computer Science, University of Tennessee, Knoxville, TN 37996 USA (e-mail: mraoufat@utk.edu; tomsovic@utk.edu; mdjouadi@utk.edu).

Color versions of one or more of the figures in this paper are available online at <http://ieeexplore.ieee.org>.

Digital Object Identifier 10.1109/TPWRS.2017.2686808

T_A	AVR time constant.
K_A	AVR excitation gain.
T_R	Time constant of the terminal voltage transducer.
V_t	Bus voltage value.
V_{ref}	Bus reference voltage value.
V_s	PSS output signal.

I. INTRODUCTION

SMALL-SIGNAL instability problems such as inter-area oscillations have become increasingly common in large power grids and may restrict the available transmission capacity between different areas [1]. In recent years, wide-area measurement systems (WAMSs) have been deployed that allow inter-area modes to be easily observed and identified [2]. As a result, low frequency oscillations can be observed globally and then appropriately designed wide-area damping controllers (WADCs) can be deployed. Many control strategies and design techniques have been reported for WADCs including designs for supplementary damping control of generators [3]–[6], renewable sources [7]–[11], high-voltage direct current (HVDC) links [12]–[14] and FACTS devices [15]–[17]. Still, the practical implementation of such WADCs face significant challenges to satisfy the reliability requirements of modern grids.

In order to transmit remote feedback signals to a WADC and then to the actuators, highly reliable communications and computations are required. Communication failures, measurement distortions, time delays or cyber-attacks can degrade the performance of the aforementioned controllers [15], [18]. Moreover, changes in scheduling of generators may mean that some actuators are temporarily unavailable. Recently, the use of doubly-fed induction generator (DFIG) wind farms for damping inter-area oscillations through active/reactive power modulation has been discussed in literatures [8], [9]. However, the availability of these weather dependent renewable resources could cause significant reliability issues. If the wind blows strongly, wind farms may efficiently contribute to damping of inter-area oscillations while on calm days the turbines may be below cut-in speeds and so actuation must come from conventional generators. Moreover, mode switching [19] may also affect the capability limits of the DFIG wind farm. Therefore, the controller should be capable of maintaining the stability and acceptable damping performance in the event of these actuator unavailabilities.

Redundancy is a common engineering approach to ensure safety, resiliency and improve overall reliability and was first introduced by Von Neumann [20]. The increase in actuator redundancy also increases the complexity of the system and

control allocation (CA) techniques are needed for distributing a given control action to individual actuators and maintaining the nominal performance under different actuator faults. Considerable research has been conducted in this area primarily for commercial and military aircraft [21]–[23], space crafts [24]–[26] and marine vessels [27], [28]. Similarly, modern power systems have been equipped with various actuators that are useful for distinct purposes. These actuators can contribute to damping inter-area oscillations (through supplementary controls) based on size of the plant (rating), operating mode, location, and how their controls impact system dynamics. We wish to take advantage of this existing built-in redundancy in power system to enhance the reliability and satisfy security requirements.

In this paper, a new modal-based control allocation (MB-CA) method is proposed to coordinate multiple actuators to optimally contribute to damping of inter-area modes and achieve a fault-tolerant WADC. In our approach, WADC is designed based on a fault-free model and the supervisory MB-CA distributes the control signals to healthy actuators based on the effects on different modes, desired control actions, total cost, and actuator limitations. This work generalizes the control allocation methods reported in [21]–[23] by considering the effects of virtual control on a modal system and extending its application to damping low-frequency oscillations in power systems. This technique allows us to give the highest priority to the control efforts associated with the critical inter-area modes. Moreover, to the best knowledge of the authors, this is the first time the control allocation concept has been applied to inter-area oscillations. This work also extends the work in [3], [4], [7]–[9] in which unavailability of a nominal WADC actuator as a result of permanent faults, maintenance, large communication delay or loss of communication has not been considered. To validate the feasibility and demonstrate the design principles, a set of comprehensive case studies are conducted on a modified 192-bus Western Electricity Coordinating Council (WECC) system with high wind penetration.

The remainder of the paper is as follows: a multi-objective LMI with pole-placement is presented in Section II as one approach for WADC design. In Section III, a modal-based control allocation method is proposed for over-actuated systems. Section IV briefly discusses the dynamic model of the test system. Time domain simulation results are provided in Section V to verify the feasibility of the proposed method and its ability to increase resiliency. Finally, concluding remarks are made in Section VI.

II. MULTI-OBJECTIVE WIDE-AREA DAMPING CONTROLLER DESIGN

In general, remote signals can provide better observability of inter-area modes and supplement the local control through WADC. We design the nominal WADC based on robust multi-objective method but our approach to CA in Section III can accommodate other methods. The linearized MIMO power system model can be written as the following generalized form

$$\dot{x}(t) = Ax(t) + Bu(t) + B_d d(t) \quad (1)$$

$$Z_\infty(t) = C_\infty x(t) + D_{\infty 2} u(t) + D_{\infty 1} d(t) \quad (2)$$

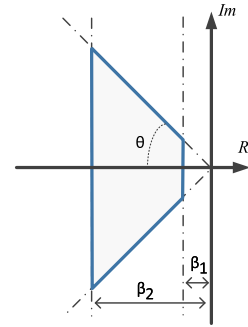


Fig. 1. Pole-placement in LMI regions.

$$Z_2(t) = C_2 x(t) + D_{22} u(t) + D_{21} d(t) \quad (3)$$

$$y(t) = Cx(t) \quad (4)$$

where $x \in R^n$, $u \in R^m$, $d \in R^q$ and $y \in R^p$ are the vector of state variables, supplementary input signals, disturbances and measured outputs. In this framework, Z_∞ channel relates to the H_∞ performance and is mainly used to guarantee robust performance against model uncertainties while Z_2 relates to the H_2 performance and guarantees satisfactory time domain performance of the system. In our study, a multi-objective damping controller was considered using the LMI optimization techniques introduced in [29] to minimize both H_2 and H_∞ norms concurrently.

Satisfactory closed loop damping can be achieved by using pole-placement objectives to force the open loop poles to lie within a proper sub-region of the left hand plane. Fig. 1 shows that pole-placement in a specified region can guarantee a minimum damping ratio of $\zeta = \cos(\theta)$ along with minimum and maximum decay rate of β_1 and β_2 . However, β_1 must be chosen as a sufficiently small number to avoid large feedback gains and the associated large control efforts. Large gains can also lead the system into saturation. Moreover, in some cases where the controller design is based on a reduced-order model, large gains can result in instability of the full-order system.

In general, our goal for WADC is to design a dynamic output feedback controller to minimize $\Gamma_1 \|T_\infty\|_\infty^2 + \Gamma_2 \|T_2\|_2^2$ along with satisfying the pole-placement requirements. Variables Γ_1 and Γ_2 are positive weightings and T_∞ and T_2 denote the transfer functions from d to Z_∞ and Z_2 , respectively. The choice of these weights depends on the particular application. The WADC can be written as:

$$\dot{\xi}(t) = A_K \xi(t) + B_K y(t) \quad (5)$$

$$\bar{u}(t) = C_K \xi(t) + D_K y(t) \quad (6)$$

where ξ and \bar{u} are WADC state vectors and outputs (damping signals). In practice, model reduction must be employed to avoid feasibility problems and to realize practical low-order controllers. In this paper, the Hankel norm approximation [30] is used to reduce the open loop model to a lower order. The order of reduction can be determined by comparing the accuracy of frequency response of the full-order and the reduced-order system in the frequency range of interest. In our approach, we design

the controller based on the reduced-order model and therefore the controller will have the same order as the reduced model.

Well-known methods such as the geometric measure of controllability gm_c and observability gm_o [3] can be used to choose the input location with the highest controllability for a specific mode and to choose the measurement signals with the highest observability regarding that mode. It is also recommended that measurement signals should have a relatively small gm_o associated with other modes to reduce interaction between different modes. In our study:

$$gm_{ci}(k) = \frac{|b_i^T \Psi_k|}{\|\Psi_k\| \|b_i\|} \quad (7)$$

$$gm_{oi}(k) = \frac{|c_i \Phi_k|}{\|\Phi_k\| \|c_i\|} \quad (8)$$

where b_i is the i th column of input matrix $B \in R^{n \times m}$ and c_i is the i th row of output matrix $C \in R^{p \times n}$. Matrices $\Psi \in R^{n \times n}$ and $\Phi \in R^{p \times n}$ are the left and right eigenvectors of matrix A , respectively.

Using this concept, outputs regarding H_∞ performance are chosen as the system outputs (measurement signals) to increase the robustness and for H_2 performance are chosen as control inputs (supplementary input signals) of the nominal WADC actuators to limit the control effort and avoid high gains in the controller. In this research, the basic steps of WADC design approach includes the following.

- 1) Perform modal analysis to identify low-frequency modes and determine the critical inter-area modes.
- 2) Select the nominal damping actuator and remote measurement based on controllability and observability measures.
- 3) Formulate the generalized plant and obtain the reduced-order model using the Hankel norm approximation.
- 4) Design the robust WADC based on the reduced-order model.
- 5) Verify and evaluate the WADC performance on the full-order model.

The next section concentrates on the MB-CA method to maintain the damping performance in the presence of actuator failures to avoid redesigning the nominal WADC.

III. MODAL-BASED CONTROL ALLOCATION

Control allocation is an approach to manage actuator redundancy and faults for an over-actuated system, where the number of actuators (m) is greater than the number of states (n). Considering the input matrix $B \in R^{n \times m}$ in (1), a group of redundant actuators $rank(B) = n < m$ needs to be available to guarantee a set of feasible control commands. In general, this assumption is not true for the full-order model of many practical systems, and in particular power grids. As a result, we consider the CA problem based on the reduced-order model described in the previous section. It is assumed that the reduced-model captures the dominant contribution of damping actuators to the low-frequency modes of interest. Using an appropriate transformation matrix $z = \psi x$ where $\psi \in R^{n \times n}$, the modal realization can be

obtained as

$$\dot{z}(t) = \Lambda z(t) + \psi Bu(t) \quad (9)$$

$$\Lambda = \begin{bmatrix} \sigma_1 & \omega_1 & 0 & \dots \\ -\omega_1 & \sigma_1 & 0 & \\ 0 & 0 & \iota_1 & \\ \vdots & & & \ddots \end{bmatrix} \quad (10)$$

where $\Lambda = \psi A \psi^{-1}$ is a block diagonal matrix having the complex eigenvalues of $\sigma_i \pm \omega_i j$ or real eigenvalue ι_i along its diagonal. Introducing a new virtual control input $v \in R^n$, (9) can be separated into two components which leads to a modular design.

$$\dot{z}(t) = \Lambda z(t) + I_n v(t) \quad (11)$$

$$v(t) = \psi Bu(t) \quad (12)$$

Virtual control $v(t)$ will be generated based on the WADC in Section II and MB-CA distributes the effort among available actuators via the command vector $u(t)$. The overall structure of the feedback loop with supervisory MB-CA is illustrated in Fig. 2. In this work, we consider analytical or model-based redundancy in the actuators as physical redundancy (e.g. replicating an actuator) is not cost effective in power systems. Given an n th-order reduced model where $n < m$, matrix ψ is full rank and $rank(\psi B) = n$. Hence, the system can now represent an over-actuated system and the resulting matrix ψB has null space of dimension $m - n$ in which u can be perturbed without significant impacts on dynamic response.

The proposed modal-based control allocation method with proper filtering to reduce the variations can be formulated as the following constrained optimization problem

$$\begin{aligned} \min_{u_t} \quad & \|W_u u_t\|^2 + \|W_s(u_t - u_{t-T_s})\|^2 \\ \text{s. t.} \quad & \psi Bu_t = v_t \\ & u_{\min} \leq u_t \leq u_{\max} \end{aligned} \quad (13)$$

where $W_u \in R^{m \times m}$ (resp. $W_s \in R^{m \times m}$) is a positive definite diagonal matrix, and represent the weighting for distributions (resp. variations) of the control signal and T_s is the time step. In the proposed method, the virtual control vector v_t (derived from the nominal WADC at time t) is distributed among all actuators considering the total cost, modal effects, actuator rates and limitations such as, saturation. This technique allows us to give the highest priority to the control efforts associated with the critical inter-area modes and obtain the feasible regions in modal coordinates.

In general, the key to control allocation is to take advantage of all the healthy actuators without having to redesign the WADC system. For power systems, the most likely actuators for damping inter-area oscillations are conventional generators, wind farms and FACTS devices equipped with supplementary control input. In case that a fault or failure occurs in the i th actuator, the i th column of matrix B can be substituted by $(1 - \Sigma)b_i$ where $\Sigma \in [0, 1]$ denotes the loss of effectiveness. For example, a complete communication failure to an actuator can be modeled by choosing $\Sigma = 1$ and the i th column will be equal to zero.

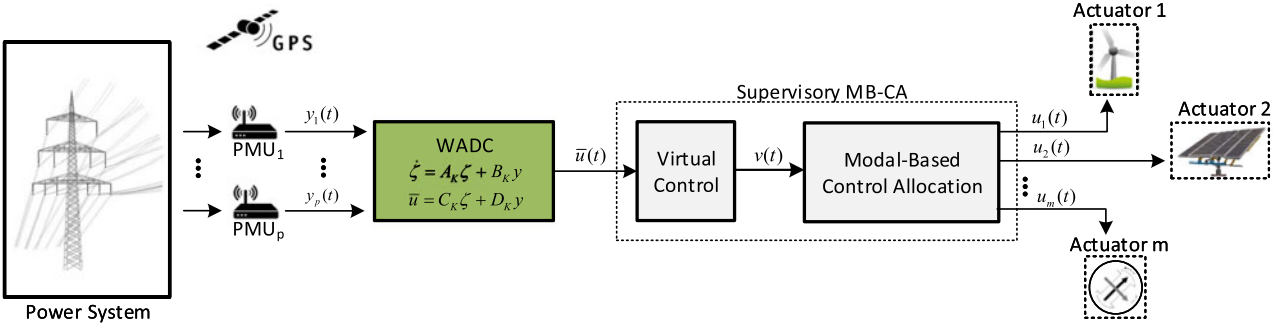


Fig. 2. Control block diagram of the feedback loop with supervisory MB-CA embedded.

To simplify the optimization problem (11), the cost function can be computed as follow and constant terms which do not affect the optimal minimizer can be omitted.

$$\begin{aligned}
& \|W_u u_t\|^2 + \|W_s(u_t - u_{t-T_s})\|^2 \\
&= u_t^T W_u^2 u_t + (u_t - u_{t-T_s})^T W_s^2 (u_t - u_{t-T_s}) \\
&= u_t^T (W_u^2 + W_s^2) u_t - 2u_t^T W_s^2 u_{t-T_s} + \text{const.} \\
&= \|W(u_t - u_d)\|^2 + \text{const.}
\end{aligned} \tag{14}$$

where

$$u_d = W_s^2 (W_u^2 + W_s^2)^{-1} u_{t-T_s}, \quad W = (W_u^2 + W_s^2)^{\frac{1}{2}} \tag{15}$$

The optimization can then be written in the form of a constrained least square problem

$$\begin{aligned}
\min_{u_t} & \|W(u_t - u_d)\|^2 \\
\text{s. t. } & \psi B u_t = v_t \\
& u_{\min} \leq u_t \leq u_{\max}
\end{aligned} \tag{16}$$

with u_d and W from (15). Utilizing the Lagrangian multiplier ρ^2 , the cost function can be expressed in the form

$$\begin{aligned}
& \|W(u_t - u_d)\|^2 + \rho^2 \|W_v(\psi B u_t - v_t)\|^2 \\
&= \left\| \begin{pmatrix} \rho W_v \psi B \\ W \end{pmatrix} u_t - \begin{pmatrix} \rho W_v v_t \\ W u_d \end{pmatrix} \right\|^2
\end{aligned} \tag{17}$$

Finally, the augmented cost function (17) yields the following optimization problem.

$$\begin{aligned}
\min_{u_t} & \left\| \begin{pmatrix} \rho W_v \psi B \\ W \end{pmatrix} u_t - \begin{pmatrix} \rho W_v v_t \\ W u_d \end{pmatrix} \right\|^2 \\
\text{s. t. } & u_{\min} \leq u_t \leq u_{\max}
\end{aligned} \tag{18}$$

Assuming there is no saturation constraint, it is possible to find the optimal distribution of control signals. With saturation constraints, the above optimization can be solved using algorithm 1 which is based on active set method [21], [31]. This algorithm can be implemented to be solved in real-time as this active set algorithm has a high efficiency given estimates of the output u_t and the set of saturated actuators \mathcal{S} are available. In our optimization problem for damping the low-frequency modes, the optimal solution at each step does not change much from the previous sampling time based on the low frequency

Algorithm 1: Active set algorithm for optimization (18).

1. Initialization:
Let $u_t = (u_{\max} + u_{\min})/2$, the set of free actuators be $\mathcal{R} := \{1, 2, \dots, m\}$ and the set of saturated actuators be $\mathcal{S} := \emptyset$
2. Main loop:
begin repeat
 Compute the unconstrained optimum in free variables:

$$\min_d \left\| \begin{pmatrix} \rho W_v \psi B \\ W \end{pmatrix} (u_t + d) - \begin{pmatrix} \rho W_v v_t \\ W u_d \end{pmatrix} \right\|^2$$
 where $d_i = 0, i \in \mathcal{R}$
 if $u_{\min} \leq u_t + d \leq u_{\max}$ **for all** \mathcal{R}
 Set $u_t = u_t + d$ and for free actuators, compute the Lagrange multiplier λ as

$$\lambda := \left(\begin{pmatrix} \rho W_v \psi B \\ W \end{pmatrix}^T \left[\begin{pmatrix} \rho W_v \psi B \\ W \end{pmatrix} u_t - \begin{pmatrix} \rho W_v v_t \\ W u_d \end{pmatrix} \right] \right)$$
 if $\mathcal{S} = \emptyset$ **or all** $\lambda \geq 0$
 Go to step 3 and vector u_t is optimal.
 else
 Move the index associated to the most negative λ from \mathcal{R} to \mathcal{S} .
 else
 Compute the maximum step length α such that $u_{\min} \leq u_t + \alpha d \leq u_{\max}$ and move the index of primary bounding constraint into \mathcal{S} .
 end
3. Hot-start:
 Use the previous optimal solution u_t and working sets \mathcal{R} and \mathcal{S} as the initial conditions in step 2.

range of the critical inter-area modes. Therefore, a hot-start can be used to initialize the optimization using the previous results and the number of iterations can be reduced significantly.

In summary, the following major steps are involved in supervisory MB-CA

- 1) Select a redundant set of actuators based on the controllability measure and identify their limits.
- 2) Choose appropriate weightings for (18).
- 3) Construct the virtual control block based on the WADC design structure to generate vector $v(t)$ from WADC.

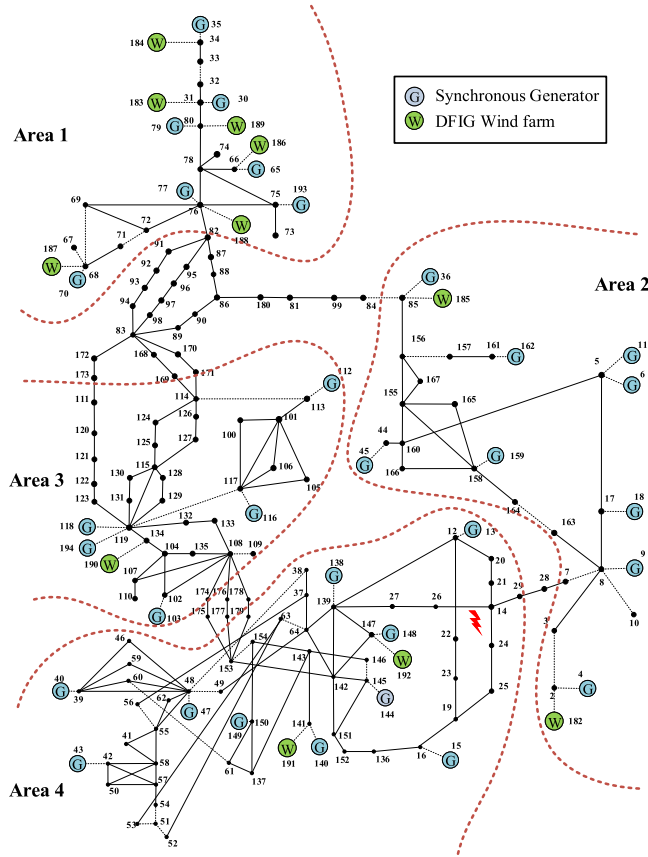


Fig. 3. Single-line diagram of the modified 192-bus WECC system with DFIG wind farms.

- 4) Design the MB-CA block based on (18) and run the algorithm 1 in real-time to obtain vector $u(t)$.
- 5) Send the control command $u_i(t)$ to the i th actuator.

IV. DYNAMIC MODEL OF THE WECC TEST SYSTEM

A modified WECC power grid with high level of wind penetration rate (20% by energy) is considered in this work to verify the effects of redundant damping actuators over low-frequency modes. Original details regarding network data, operating conditions and dynamic parameters are given in [32]. The system with WECC boundaries can be seen in Fig. 3. It consists of 31 conventional generators with total generation of 48.49 GW and 11 wind farms with generation of 13.5 GW. Loads are considered to be constant power. In the following, dynamic models of different actuator components equipped with supplementary control inputs are outlined to formulate the problem of actuator constraints and failures.

A. Generator Dynamic Model

Generators are represented by a two-axis model [33]:

$$\dot{\delta} = \omega - \omega_s \quad (19)$$

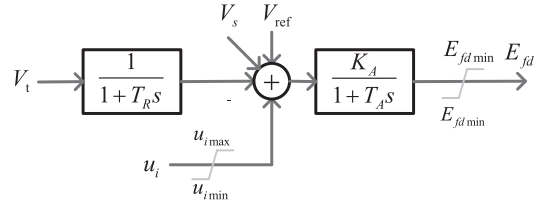


Fig. 4. Schematic of the high-gain AVR system with supplementary input u .

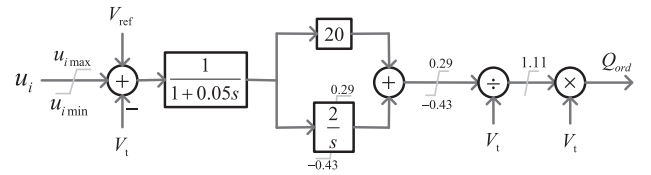


Fig. 5. Schematic of DFIG reactive power control loop with supplementary input u .

$$\begin{aligned} \frac{2H}{\omega_s} \dot{\omega} &= T_M - I_d E'_d - I_q E'_q \\ &\quad - (X'_q - X'_d) I_q I_d - D(\omega - \omega_s) \end{aligned} \quad (20)$$

$$T'_q \dot{E}'_d = -E'_d + (X_q - X'_q) I_q \quad (21)$$

$$T'_d \dot{E}'_q = -E'_q - (X_d - X'_d) I_d + E_{fd} \quad (22)$$

The notation is as defined in the Nomenclature. Standard speed-based PSS model (PSS1A) [34] is used to improve damping of the local modes and governors are modeled by the IEEEG1 steam turbine model [35].

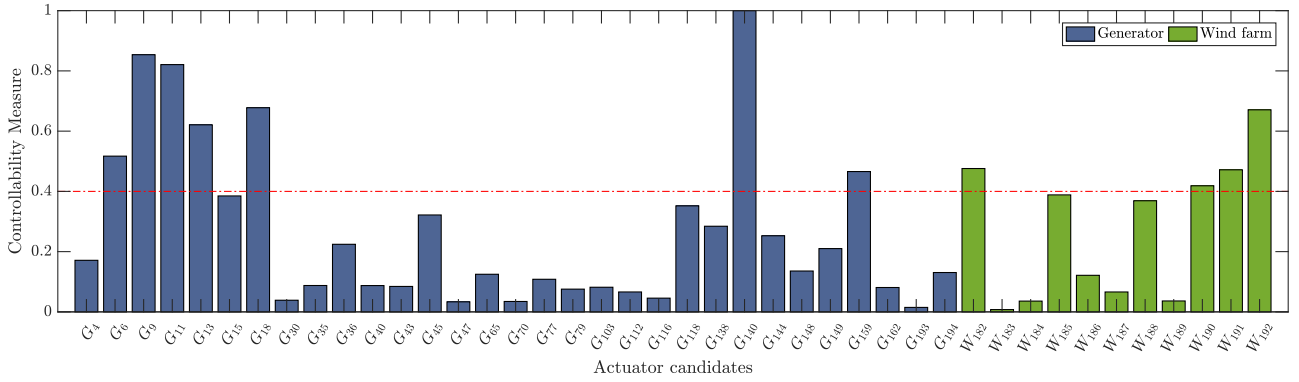
The generators are assumed to be equipped with high-gain AVR systems and supplementary control inputs as shown in Fig. 4. Saturation nonlinearity on the field voltage E_{fd} is also considered in the design process. In high-gain excitation systems, typical values of time constant T_A are in the range of 0.01 – 0.05 s. Therefore, T_A is negligible and limits on the field voltage can be modeled by limits of $K_A^{-1} E_{fd\min} - K_A^{-1} E_{fd\max}$ pu on the output of summation block. As a result, the following saturation limits can be considered on the supplementary input u_i .

$$\eta K_A^{-1} E_{fd\min} \leq u_i \leq \eta K_A^{-1} E_{fd\max} \quad (23)$$

where $\eta \in [0, 1]$ should be chosen to allow an acceptable control range and provide adequate damping while prevent tripping of the generator. Moreover, these limits also minimize the negative effects of damping controllers on voltage regulatory response and are usually in the range of ± 0.05 to ± 0.1 pu which guarantees a modest level of contribution.

B. DFIG-Based Wind Farm Model

A large wind farm may consist of several hundred DFIG wind turbines. Representing each individual unit in the wind farm model can be difficult and unnecessary for large system studies. By aggregation, an equivalent lumped model of a wind farm can be represented by a large DFIG. In this work, the base power of each wind farm is scaled based on the total number of



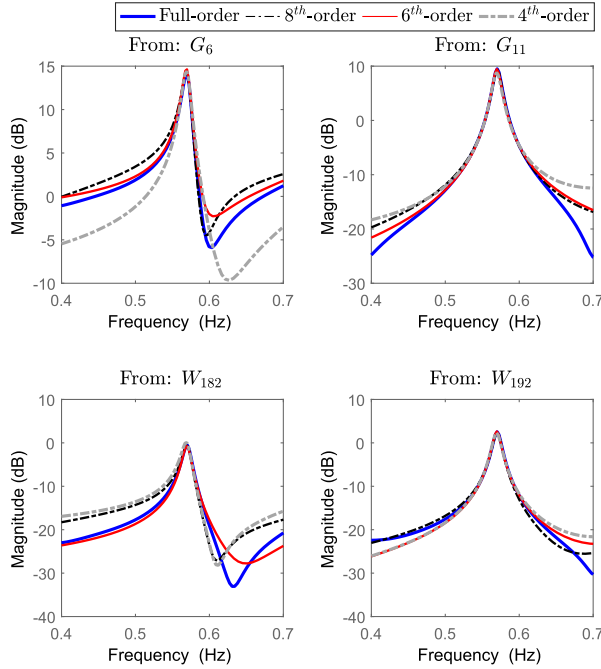


Fig. 8. Frequency response of the full-order and reduced-order models of the WECC system from supplementary inputs.

mode 3 and has a close frequency response to the full-order system for interesting input candidates. The nominal WADC is designed based on the 6th-order model to meet or exceed 7% damping mainly over the critical mode 3. The design parameters of the multi-objective WADC are given as $\Gamma_1 = 1$, $\Gamma_2 = 10$, $\beta_1 = -0.005$, $\beta_2 = -50$. The controller matrices can be found in Appendix B. The choice of design variables usually depends upon the individual application and design requirements, such as, low control effort. Table I also shows a significant improvement in damping ratio of the critical mode 3 with WADC while only slightly affecting the other modes. Since MB-CA offers the advantages of modular design, the output of the WADC controller $\bar{u}(t)$ can be used to generate the virtual control vector $v(t) = \psi b_6 \bar{u}(t)$. This block is just a gain matrix and depends on the WADC design structure.

C. Design of Modal-Based Control Allocation

The proposed MB-CA is implemented as a user-defined model (UDM) [36] in TSAT [39] by using dynamically linked blocks (DLBs) and the optimization algorithm 1 is implemented using C/C++ with fixed time step of $T_s = 0.02$ s. The weighting functions and gains are chosen as follows: $W_u := \text{diag}(1, 1, 1, 1, 1, 0.5, 1, 1, 1, 1, 1)$, $W_s := 5W_u$, $W_v := \text{diag}(2, 2, 4, 4, 8, 8)$ and $\rho := 10$. The weighting W_u is chosen such that deviation of the nominal actuator is penalizing less than other actuators. This choice of weighting matrix prioritizes the use of the nominal WADC actuator in normal condition to reduce the cost. Moreover, the choice of W_v gives the highest priority to the control efforts regarding the critical mode 3. We choose $T_R = 0$, $T_A = 0.02$, $K_A = 50$, $\eta = 0.5$, $E_{fd\max} = -E_{fd\min} = 7.5$ pu so hard limits for the generators are $u_{\max} = -u_{\min} = 0.075$ pu. Additionally, hard limits

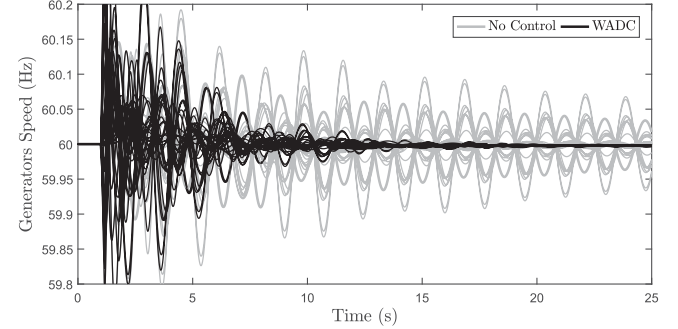


Fig. 9. Dynamic response of the system to three-phase fault at bus #14.

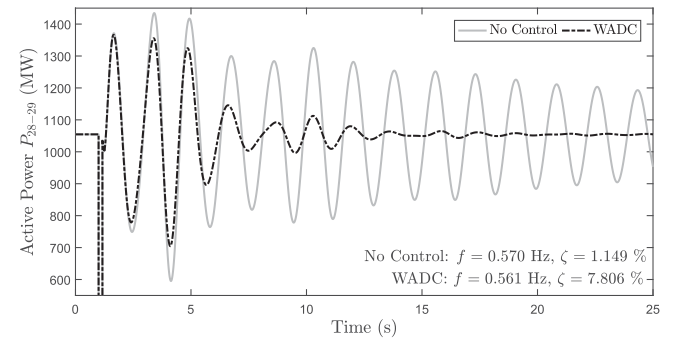


Fig. 10. Power flow on the tie-line connecting the areas 2 and 4 after a three-phase fault at bus #14.

of $u_{\max} = -u_{\min} = 0.1$ pu are imposed on the supplementary damping signals of wind farms.

D. Discussion

Nonlinear time domain simulations are conducted using TSAT program. Different variables are monitored and Prony analysis is performed based on the nonlinear response to estimate damping ratio and frequency of the critical modes. To evaluate the performance, different faults are considered in both actuators and the physical system. A symmetrical three-phase fault is applied to bus #14 (marked in Fig. 3) near the tie-line connecting the areas 2 and 4. The fault occurs at $t = 1$ s and is cleared after 10 cycles. In this study, the time frame of analysis (oscillation) is restricted to a few seconds and so reasonable to assume that the wind speed remains constant throughout the simulation period.

Without control allocation, the system responses are as been shown in Figs. 9 and 10. Using Prony analysis of the nonlinear response, it can be observed that WADC can significantly improve the damping from 1.149% to 7.806%. If there is any failure in the nominal WADC actuator, the system will illustrate a similar response to the no control system with damping of 1.149%. Note that results from Prony analysis are slightly different from the linearized results in Table I because of the nonlinear nature of the system.

In case with modal-based control allocation, the system responses are shown in Figs. 11 and 12 for the following cases.

- 1) *Case A:* No faulty actuators $\mathcal{F} = \{\emptyset\}$;
- 2) *Case B:* Faults in the nominal actuator $\mathcal{F} = \{G_{140}\}$, hard limits $u_{\max} = -u_{\min} = 0.05$ pu for all wind farms;

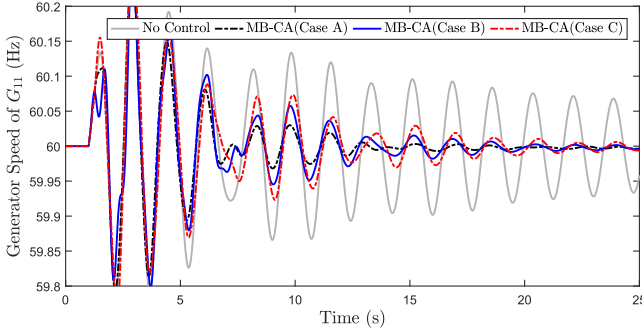


Fig. 11. Dynamic response of the system to three-phase fault at bus #14 when MB-CA redirects the WADC signal to healthy actuators.

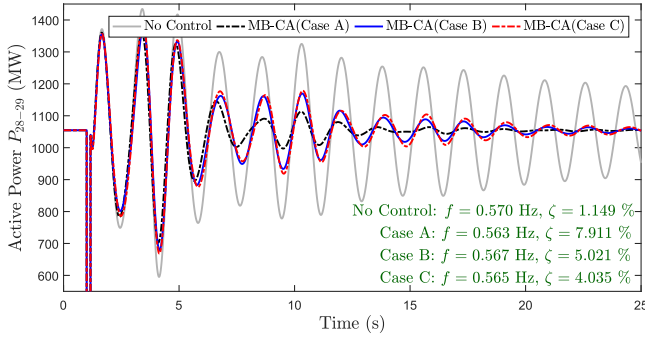


Fig. 12. Power flow on the tie-line connecting areas 2 and 4 to a three-phase fault at bus #14 when MB-CA redirects WADC signal to healthy actuators.

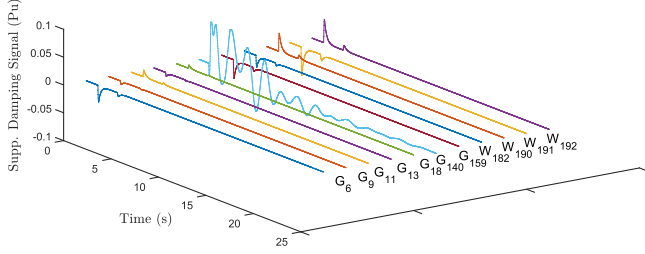


Fig. 13. Supplementary signals (MB-CA outputs) in Case A.

3) *Case C*: Faults in six random actuators $\mathcal{F} = \{G_6, G_{13}, G_{18}, G_{140}, W_{182}, W_{192}\}$;

It can be seen that in case A, where there is no faulty actuator, MB-CA mainly use the nominal damping actuators and can compensate the effects of hard limits on the actuators. In case B, the nominal WADC actuator suffers a loss of communication and hard limits on wind farms are narrowed by 50%. MB-CA successfully recovers the performance of the system. In case C, where more than half of the actuators have failed, the wind farm W_{182} is disconnected and the rest face a communication failure, MB-CA will damp the oscillations by distributing the control signal to healthy actuators and maintain a sufficient damping of 4.035%. Comparing these results, it can be seen that even though the damping performance in case C is not as good as Case A and B, it is far better than without MB-CA. The proposed method clearly enhances fault tolerance of the WADC system. Figs. 13, 14 and 15 illustrate the MB-CA outputs in

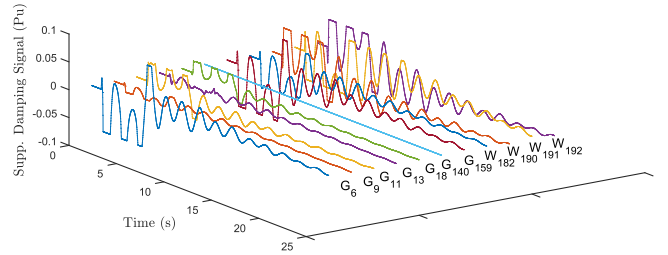


Fig. 14. Supplementary signals (MB-CA outputs) in Case B.

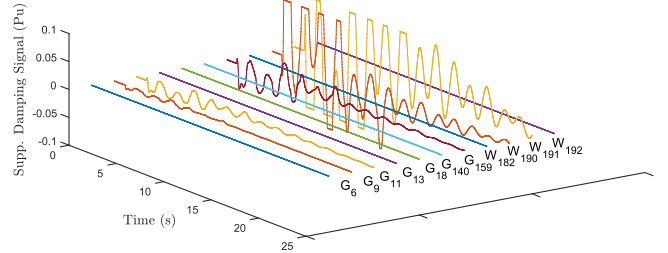


Fig. 15. Supplementary signals (MB-CA outputs) in Case C.

TABLE II
DAMPING RATIO OF MODE 3 WITH RESPECT TO DIFFERENT CONTROLLERS AND FAULT COMBINATIONS

Faulty Actuator Set \mathcal{F}	Damping Ratio (%)		
	MB-CA	CA	WADC
\emptyset	7.911	7.907	7.806
G_{140}	5.052	4.759	1.149
G_6, G_{140}	4.950	4.624	1.149
G_6, G_{140}, W_{182}	4.899	4.353	1.149
$G_6, G_{18}, G_{140}, W_{182}$	4.316	3.744	1.149
$G_6, G_{18}, G_{140}, W_{182}, W_{192}$	4.086	3.103	1.149
$G_6, G_{18}, G_{140}, W_{182}, W_{190}, W_{192}$	3.817	2.949	1.149
$G_6, G_{11}, G_{18}, G_{140}, W_{182}, W_{192}$	3.329	1.467	1.149

Case A, B and C, respectively and effects of actuator faults and limits are clearly observed.

Various results with respect to different controllers and fault combinations are included in Table II. In all cases, the nominal WADC actuator G_{140} is assumed to be faulty. It is shown that the proposed MB-CA tolerates multiple failures and maintains the minimum acceptable damping of 3.329% over the critical mode in compare to 1.467% damping in case where all modes have identical weights. In general, the optimal solution may not be feasible for all virtual control inputs, constraints and failures. Fig. 16 visualizes the average feasible virtual control regions in modal coordinates for the critical mode 3 considering all failure scenarios. These regions can be obtained considering the actuator constraints in (13) and provides insight to the degree of fault tolerance. Different faults in the actuators or adding more constraints can further reduce the area of feasible region, which is related to the attainable damping ratio.

In this work, the previous optimization results are used as the starting point to solve the MB-CA problem for the next sampling time. Fig. 17 depicts the distribution of the number of iterations required by the algorithm in Case B, with and without

$$A_K = \begin{bmatrix} -0.757 & 0.460 & -0.343 & 6.254 & 0.182 & -0.405 \\ -0.460 & -0.144 & 5.981 & -2.658 & -0.173 & 0.320 \\ -0.343 & -5.981 & -0.244 & 19.66 & 0.195 & -0.488 \\ -6.254 & -2.658 & -19.66 & -51.20 & -4.252 & 7.237 \\ 0.182 & 0.173 & 0.195 & 4.252 & -0.501 & 6.998 \\ 0.405 & 0.320 & 0.488 & 7.237 & -6.998 & -3.321 \end{bmatrix}, B_K = \begin{bmatrix} -1.682 \\ -0.376 \\ -0.475 \\ -5.745 \\ 0.207 \\ 0.443 \end{bmatrix}, C_K = \begin{bmatrix} -1.682 \\ 0.376 \\ -0.475 \\ 5.745 \\ 0.207 \\ -0.443 \end{bmatrix}^T, D_K = 0 \quad (25)$$

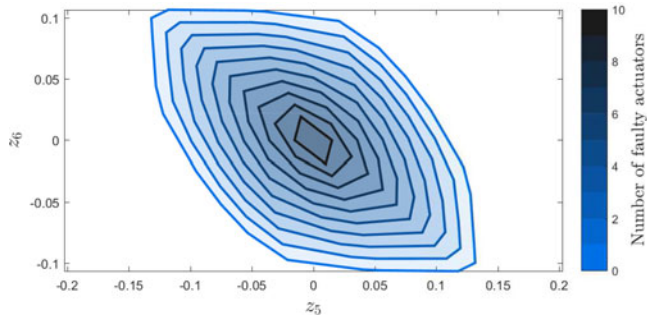


Fig. 16. Effects of actuator faults on feasible virtual control region for inter-area mode 3.

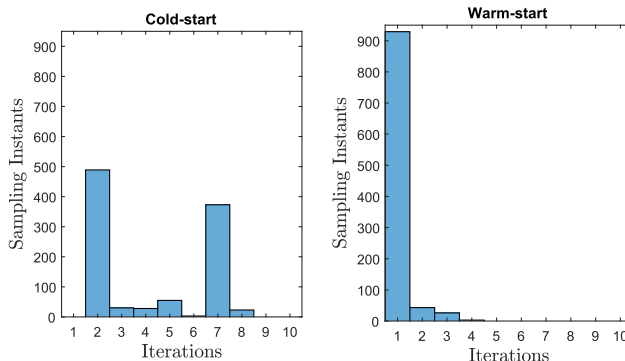


Fig. 17. Histogram showing the number of iterations required by the optimization algorithm in Case B from $t = 1$ s to $t = 6$ s.

warm-start. It clearly indicates that in case of warm-start, the algorithm can converge mostly in one iterations and significantly improve the performance.

VI. CONCLUSION

In this paper, a new approach to designing a fault-tolerant WADC using modal-based control allocation is proposed to coordinate a group of actuators to optimally contribute to damping of inter-area oscillations. In our proposed method when an actuator fails or is unavailable, the supervisory MB-CA distributes the control signals to the remaining healthy actuators based on the effects on modal system, the desired control action and actuator constraints. The WADC design is carried out using multi-objective H_2/H_∞ optimization with pole-placement region to achieve high damping performance. In the next step, the MB-CA is designed to manage actuator failures and constraints without redesigning the nominal WADC. The feasibility and performance of the proposed method is analyzed using the WECC system. Numerical results have verified the effectiveness of the

TABLE III
DFIG WIND FARMS OUTPUTS IN THE WECC TEST SYSTEM

Bus No.	Base MVA	MW	MVAr	PF
182	600	400	-114	-0.96
183	1500	1062	164	0.98
184	1410	1000	175	0.98
185	1050	700	41	0.99
186	1410	1000	-317	-0.95
187	1140	880	183	0.97
188	3600	2369	576	0.97
189	3600	3000	423	0.99
190	1500	1068	-36	-0.99
191	1500	1050	235	0.97
192	1350	980	148	0.98

proposed method to provide sufficient damping and build in resiliency to different faults.

APPENDIX A

Table III provides the wind generation in the numerical simulations.

APPENDIX B

The balanced WADC controller matrices are given in (25) at the top of the page.

REFERENCES

- [1] Y. Zhang, M. E. Raoufat, and K. Tomsovic, "Remedial action schemes and defense systems," in *Smart Grid Handbook*. Hoboken, NJ, USA: Wiley, 2016.
- [2] I. Kamwa, R. Grondin, and Y. Hébert, "Wide-area measurement based stabilizing control of large power systems-a decentralized/hierarchical approach," *IEEE Trans. Power Syst.*, vol. 16, no. 1, pp. 136–153, Feb. 2001.
- [3] Y. Zhang and A. Bose, "Design of wide-area damping controllers for interarea oscillations," *IEEE Trans. Power Syst.*, vol. 23, no. 3, pp. 1136–1143, Aug. 2008.
- [4] F. Dörfler, M. R. Jovanović, M. Chertkov, and F. Bullo, "Sparsity-promoting optimal wide-area control of power networks," *IEEE Trans. Power Syst.*, vol. 29, no. 5, pp. 2281–2291, Sep. 2014.
- [5] M. E. Raoufat, K. Tomsovic, and S. M. Djouadi, "Power system supplementary damping controllers in the presence of saturation," in *Proc. 2017 IEEE Power Energy Conf. Illinois (PECI)*, Champaign, IL, USA, 2017.
- [6] M. E. Raoufat, K. Tomsovic, and S. M. Djouadi, "Virtual actuators for wide-area damping control of power systems," *IEEE Trans. Power Syst.*, vol. 31, no. 6, pp. 4703–4711, Nov. 2016.
- [7] A. E. Leon and J. A. Solsona, "Power oscillation damping improvement by adding multiple wind farms to wide-area coordinating controls," *IEEE Trans. Power Syst.*, vol. 29, no. 3, pp. 1356–1364, May 2014.
- [8] M. Mokhtari and F. Aminifar, "Toward wide-area oscillation control through doubly-fed induction generator wind farms," *IEEE Trans. Power Syst.*, vol. 29, no. 6, pp. 2985–2992, Nov. 2014.
- [9] L. Fan, H. Yin, and Z. Miao, "On active/reactive power modulation of DFIG-based wind generation for interarea oscillation damping" *IEEE Trans. Energy Convers.*, vol. 26, no. 2, pp. 513–521, Jun. 2011.

- [10] R. Shah, N. Mithulananthan, K. Y. Lee, and R. C. Bansal, "Wide-area measurement signal-based stabilizer for large-scale photovoltaic plants with high variability and uncertainty," *IET Renew. Power Gener.*, vol. 7, pp. 614–622, 2013.
- [11] R. Shah, N. Mithulananthan, and K. Y. Lee, "Large-scale PV plant with a robust controller considering power oscillation damping," *IEEE Trans. Energy Convers.*, vol. 28, no. 1, pp. 106–116, Mar. 2013.
- [12] J. He, C. Lu, X. Wu, P. Li, and J. Wu, "Design and experiment of wide area HVDC supplementary damping controller considering time delay in China southern power grid," *IET Gener., Transm. Distrib.*, vol. 3, pp. 17–25, 2009.
- [13] W. Juanjuan, F. Chuang, and Z. Yao, "Design of WAMS-based multiple HVDC damping control system," *IEEE Trans. Smart Grid*, vol. 2, no. 2, pp. 363–374, Jun. 2011.
- [14] R. Preece, J. V. Milanović, A. M. Almutairi, and O. Marjanovic, "Damping of inter-area oscillations in mixed AC/DC networks using WAMS based supplementary controller," *IEEE Trans. Power Syst.*, vol. 28, no. 2, pp. 1160–1169, May 2013.
- [15] W. Yao, L. Jiang, J. Wen, Q. H. Wu, and S. Cheng, "Wide-area damping controller of FACTS devices for inter-area oscillations considering communication time delays," *IEEE Trans. Power Syst.*, vol. 29, no. 1, pp. 318–329, Jan. 2014.
- [16] J. Deng, C. Li, and X. P. Zhang, "Coordinated design of multiple robust FACTS damping controllers: A BMI-based sequential approach with multi-model systems," *IEEE Trans. Power Syst.*, vol. 30, no. 6, pp. 3150–3159, Nov. 2015.
- [17] Y. Li, C. Rehtanz, S. Ruberg, L. Luo, and Y. Cao, "Wide-area robust coordination approach of HVDC and FACTS controllers for damping multiple interarea oscillations," *IEEE Trans. Power Del.*, vol. 27, no. 3, pp. 1096–1105, Jul. 2012.
- [18] S. Zhang and V. Vitali, "Design of wide-area power system damping controllers resilient to communication failures," *IEEE Trans. Power Syst.*, vol. 28, no. 4, pp. 4292–4300, Nov. 2013.
- [19] Y. Zhang, K. Tomsovic, S. M. Djouadi, and H. Pulgar-Painemal, "Hybrid controller for wind turbine generators to ensure adequate frequency response in power networks," *IEEE J. Emerg. Sel. Topics Circuits Syst.*, vol. PP, no. 99, pp. 1–12, Mar. 2017.
- [20] J. Von Neumann, "Probabilistic logics and the synthesis of reliable organisms from unreliable components," *Automata Stud.*, vol. 34, pp. 43–98, 1956.
- [21] O. Härkegård, "Efficient active set algorithms for solving constrained least squares problems in aircraft control allocation," in *Proc. IEEE Conf. Decis. Control*, vol. 2, pp. 1295–1300, 2002.
- [22] O. Härkegård and S. T. Glad, "Resolving actuator redundancy-optimal control versus control allocation," *Automatica*, vol. 41, pp. 137–144, 2005.
- [23] H. Alwi and C. Edwards, "Fault tolerant control using sliding modes with on-line control allocation," *Automatica*, vol. 44, pp. 1859–1866, 2008.
- [24] P. A. Servidio and R. S. Pena, "Spacecraft thruster control allocation problems," *IEEE Trans. Autom. Control*, vol. 50, no. 2, pp. 245–249, Feb. 2005.
- [25] J. Jin, B. Park, Y. Park, and M.-J. Tahk, "Attitude control of a satellite with redundant thrusters," *Aerospace Sci. Technol.*, vol. 10, pp. 644–651, 2006.
- [26] Q. Shen, D. Wang, S. Zhu, and E. K. Poh, "Inertia-free fault-tolerant spacecraft attitude tracking using control allocation," *Automatica*, vol. 62, pp. 114–121, 2015.
- [27] O. J. Sordalen, "Optimal thrust allocation for marine vessels," *Control Eng. Pract.*, vol. 5, pp. 1223–1231, 1997.
- [28] T. I. Fossen and T. A. Johansen, "A survey of control allocation methods for ships and underwater vehicles," in *Proc. 14th Mediterranean Conf. Control Autom.*, pp. 1–6, 2006.
- [29] C. Scherer, P. Gahinet, and M. Chilali, "Multiobjective output-feedback control via LMI optimization," *IEEE Trans. Autom. Control*, vol. AC-42, no. 7, pp. 896–911, Jul. 1997.
- [30] K. Glover, "All optimal Hankel-norm approximations of linear multi-variable systems and their L_∞ -error bounds," *Int. J. Control*, vol. 39, pp. 1115–1193, 1984.
- [31] Å. Björck, *Numerical Methods for Least Squares Problems*. Philadelphia, PA, USA: SIAM, 1996.
- [32] "Test cases library of sustained power system oscillations." [Online]. Available: <http://web.eecs.utk.edu/~kaisun/Oscillation/>
- [33] J. Machowski and J. R. Bumby, *Power System Dynamics and Stability*. New York, NY, USA: Wiley, 1997.
- [34] *IEEE Recommended Practice for Excitation System Models for Power System Stability Studies*, IEEE Std. 421.5-2005, pp. 1–85, 2006.
- [35] P. Pourbeik *et al.*, "Dynamic models for turbine-governors in power system studies," in *IEEE Task Force on Turbine-Governor Modeling*, Jan. 2013.
- [36] Powertech, *DSATools User-Defined Model (UDM) User Manual*. Powertech Labs Inc., Surrey, BC, Canada, 2012.
- [37] Y. Liu, K. Sun, and Y. Liu, "A measurement-based power system model for dynamic response estimation and instability warning," *Elect. Power Syst. Res.*, vol. 124, pp. 1–9, 2015.
- [38] Powertech, *Small Signal Analysis Tool (SSAT) User Manual*. Powertech Labs Inc., Surrey, BC, Canada, 2012.
- [39] Powertech, *Transient Security Assessment Tool (TSAT) User Manual*. Powertech Labs Inc., Surrey, BC, Canada, 2012.



M. Ehsan Raoufat (S'11) received the B.S. and M.S. degrees from Shiraz University, Shiraz, Iran, in 2009 and 2011, respectively. He is currently working toward the Ph.D. degree in the Department of Electrical Engineering and Computer science, University of Tennessee, Knoxville, TN, USA.

His main research interests include distributed, decentralized, and stochastic control with their applications to large-scale power systems and smart grids.



Kevin Tomsovic (F'07) received the B.S. degree in electrical engineering from Michigan Technological University, Houghton, MI, USA, in 1982, and the M.S. and Ph.D. degrees in electrical engineering from the University of Washington, Seattle, WA, USA, in 1984 and 1987, respectively.

He is currently a CTI Professor in the Department of Electrical Engineering and Computer Science, University of Tennessee, Knoxville, TN, USA, where he also directs the NSF/DOE sponsored ERC CURENT. He was on the faculty of Washington State

University from 1992–2008. He held the Advanced Technology for Electrical Energy Chair at Kumamoto University, Kumamoto, Japan, from 1999 to 2000 and was an NSF Program Director in the ECS Division of the Engineering Directorate from 2004 to 2006.



Seddik M. Djouadi (M'99) received the B.S. degree (with First Class Hons.) from the Ecole Nationale Polytechnique, El-Harrach, Algiers, the M.Sc. degree from the University of Montreal, Montreal, QC, Canada, and the Ph.D. degree from McGill University, Montreal, QC, Canada, all in electrical engineering, in 1989, 1999, and 1992, respectively.

He is currently a Full Professor in the Electrical Engineering and Computer Science Department, University of Tennessee, Knoxville, TN, USA. Prior to joining the University of Tennessee, he was an As-

sistant Professor in the University of Arkansas at Little Rock, Little Rock, AR, USA, and held postdoctoral positions in the Air Force Research Laboratory and Georgia Institute of Technology, where he was also a Design Engineer with American Flywheel Systems Inc. His research has been supported by the National Science Foundation, Oak Ridge National Laboratory, the Air Force Office of Scientific Research, and the Tennessee Valley Authority. His research interests include filtering and control of systems under communication constraints, modeling and control of wireless networks, control systems and applications to autonomous sensor platforms, electromechanical and mobile communication systems, in particular smart grid and power systems, control systems through communication links, networked control systems, and model reduction for aerodynamic feedback flow control.

Dr. Djouadi received five US Air Force Summer Faculty Fellowships, and five Oak Ridge National Laboratory Summer Fellowships. He received the Best Paper Award in the 1st Conference on Intelligent Systems and Automation 2008, the Ralph E. Powe Junior Faculty Enhancement Award in 2005, the Tibbet Award with AFS Inc. in 1999, and the American Control Conference Best Student Paper Certificate (best five in competition) in 1998. He was selected by Automatica twice as an outstanding reviewer for 2002–2003 and 2003–2004.